2000

Condensation Heat Transfer of New Refrigerants: Advantages of High Pressure Fluids

A. Cavallini
Universita de Padova

D. Del Col
Universita de Padova

L. Doretti
Universita de Padova

L. Rossetto
Universita de Padova

G. A. Longo
Universita de Padova

CONDENSATION HEAT TRANSFER OF NEW REFRIGERANTS: ADVANTAGES OF HIGH PRESSURE FLUIDS

A. Cavallini, D. Del Col, L. Doretti, L. Rossetto
Dipartimento di Fisica Tecnica
Università di Padova
Via Venezia 1, I-35131 Padova - Italy

G. A. Longo
Dipartimento di Tecnica e Gestione dei Sistemi Industriali
Università di Padova
Viale X Giugno 22, I-36100 Vicenza - Italy

ABSTRACT

Heat transfer condensation tests inside a 8 mm ID tube for R-134a, R-410A and R-125 are reported at an average saturation temperature of 40°C, at mass velocities ranging from 65 to 750 kg/(m^2 s), over the entire vapour quality range. After comparing the experimental data against a model able to predict both shear force and gravity driven condensation, a comparison among these fluids has been carried out. Drop in saturation temperature is chosen as the benchmark, with R-22 as the reference fluid, to show advantages of high pressure fluids regarding heat transfer performance.

NOMENCLATURE

D	diameter [m]	ρ	density [kg/m^3]
DT	temperature difference ($T_{sat} - T_W$) [K]	**Subscripts**	
G	mass velocity [kg/(m^2 s)]	CALC	calculated
h	heat transfer coefficient [W/(m^2 K)]	DR	driving
i_{LG}	latent heat [J/kg]	EXP	experimental
p	pressure [Pa]	f	friction
q	heat flow rate [W]	G	gas phase
T	temperature [K]	L	liquid phase
x	vapour quality	sat	saturation
z	axial coordinate [m]	w	tube wall

INTRODUCTION

The phase out of R-22, the most used refrigerant in the air conditioning industry, is underway in Europe, as old-generation refrigerants are thought to be major contributors to the depletion of the stratospheric ozone layer (Montreal Protocol). Some promising substitutes for refrigerant 22 are zeotropic mixtures of HFC fluids, which present a considerable heat transfer penalty due to mass transfer thermal resistance build-up in two-phase processes. Alternatively both pure fluids and near-azeotropic HFC mixtures (such as R410A) can be used, which on the other hand may display a high operating pressure. When the substitution for traditional ozone-depleting refrigerants involves the use of high pressure fluids, this usually implies a reduction of friction losses, with higher energetic performance, and a reduction of the size of the plant.

The aim of this work is to investigate the condensation performance (which involves both heat transfer and drop in saturation temperature) of new high pressure HFC refrigerants. The authors present their own data for R-134a, R-410A and R-125 during condensation. These tests cover a wide range of operating pressures, from 1 MPa for R-134a up to 2.5 MPa in the case of R-410A.

It is well known that a correct evaluation of heat transfer performance of new refrigerants requires an accurate knowledge of their pressure drop behavior. Several correlations have been proposed in the past for predicting two-phase pressure drop inside smooth tubes, and particularly for computing the two-phase frictional multipliers. Besides, present authors show the predictibility of the heat transfer coefficients for such new fluids by relating the heat transfer to the friction pressure gradient, as shown in the past by Kosky and Staub (1971) and by Traviss et al. (1972) for CFC and HCFC fluids.

EXPERIMENTAL FACILITY

The experimental tests are run at the Dipartimento di Fisica Tecnica of the University of Padova. The test section is a counter flow double tube condenser, with the refrigerant condensing in the inner tube, against cold water flowing in the annulus. The test section includes a pre-condensing section, around 300 mm long, where the refrigerant achieves a fully developed flow regime, and the measuring section, a 8 mm inside diameter smooth tube around 1.0 m long, instrumented with thermocouples embedded in the tube wall to measure the wall temperature.

A schematic view of the apparatus is provided in Figure 1. It consists of three loops: the refrigerant loop, the cooling water loop and the hot water loop. In the primary loop the refrigerant is vapourised and superheated in two tube-in-tube heat exchangers placed in series, heated by hot water. Then the refrigerant partially condenses in the precondenser to achieve the set quality at the inlet of the test section.

Refrigerant temperatures at inlet and outlet of the test tube are measured by means of adiabatic sections, using thermocouples inserted into both the refrigerant flow and the tube wall. The two-phase mixture leaves the test section and goes to an after-condenser, a braised plate type condenser, where it is fully condensed and sub-cooled. The refrigerant flow can be independently controlled by a variable stroke volumetric pump. Two digital strain gauge pressure transducers (absolute and differential transducers) are connected to manometric taps to measure the vapour pressure upstream and downstream of the test tube.

The refrigerant mass flow rate is measured by a Coriolis effect mass flow meter, inserted downstream of the pump, having an accuracy of 0.4% of the measured value. The cooling water is kept at constant temperature in a forced convection loop. Its flow rate is measured by a magnetic-type flow meter and its temperature gain across the instrumented test tube is measured with a differential copper-constantan thermopile, installed into mixing chambers to assure perfect mixing of the water. The average accuracy of the thermocouples is estimated to be equal to 0.05°C. For the thermopiles, the average accuracy is around 0.03°C. It was estimated from a propagation of error analysis that the heat transfer coefficients were measured to an accuracy of ± 5.0 % at typical test conditions. A list of accuracy for sensors and parameters is reported in Table 1.

EXPERIMENTAL HEAT TRANSFER RESULTS

The heat flux exchanged in the test tube is derived from a thermal balance on the cooling water side. The average condensation heat transfer coefficient is obtained as:

$$h = q / (A\, \Delta T_{ln}) \qquad (1)$$

where q is the heat flux exchanged in the test tube, A is the exchange surface area and ΔT_{ln} is the logarithmic average temperature difference between the vapour and the tube wall. The vapour quality entering the test section (x_{in}) is calculated from an energy balance on the precondenser. For pure refrigerants (R-134a, R-125) or the nearly azeotropic mixture R-410A, the vapour quality change is given as a ratio of the isobaric change in enthalpy in the test section to the latent heat.

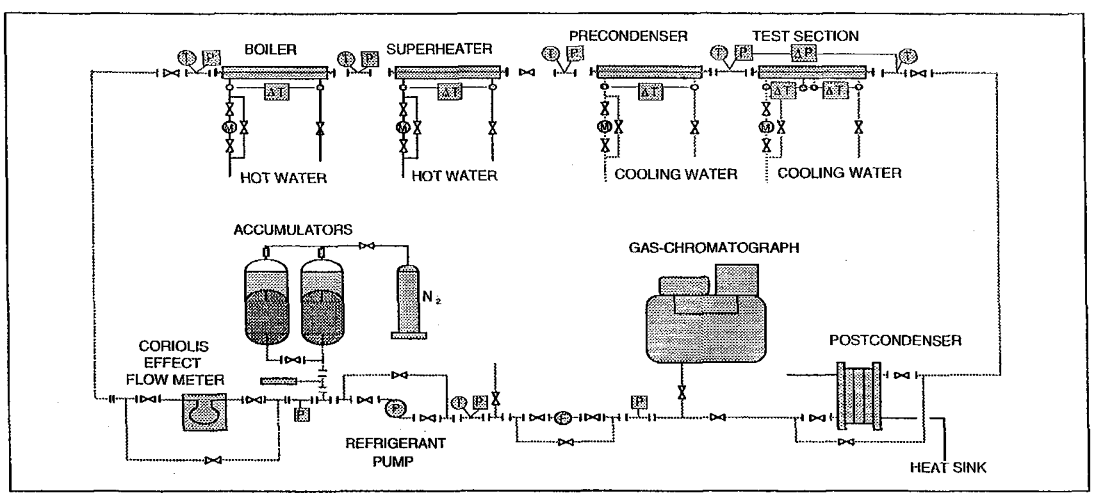

Figure 1. Schematic view of the experimental rig.

Table 1: Accuracy for sensors and parameters

Temperature	± 0.05°C	Temperature difference	± 0.03°C
Refrigerant flow rate	± 0.4%	Absolute pressure	± 0.1% f.s.
Water flow rate	± 1.5%	Heat flow rate	± 4.5%
Vapour quality	± 0.05	Heat transfer coefficient	± 5.0%

R-134a condensation tests are carried out at 40 ± 3°C saturation temperature, with a saturation pressure of 1020 kPa. The average inlet vapour quality varies between 0.2 and 0.9, and approximately 15 – 25% vapour quality change occurs in the test tube depending on the mass flux velocity and heat flux. The heat transfer values presented are actually mean values over a small change of vapour quality and can be referred to as quasi-local values. Figure 2 shows the condensation heat transfer for R-134a plotted as a function of the vapour quality at mass velocities equal to 65, 100, 200, 300, 400 and 750 kg/(m^2 s) (in the figure mass velocity is referred to as G). The figure shows that the condensation heat transfer coefficient increases with increasing mass velocity and vapour quality. At low mass velocity (65 and 100 kg/(m^2 s)), there is a very light dependence of heat transfer coefficient on vapour quality. This trend suggests that the vapour shear forces in these situations are almost negligible and the flow pattern is stratified. At this mass velocity, on the contrary, it is observed a strong effect of the temperature difference between saturation and wall (indicate as DT in the figure), in accordance with the Nusselt theory for gravity driven condensation. As the mass velocity increases, although the flow patterns may remain basically stratified, the vapour shear forces become more and more significant and this results in a higher slope for the trend of heat transfer coefficient against vapour quality. At higher flow rates (400 and 750 kg/(m^2 s)) the condensation coefficient shows a linear trend and a higher slope against the vapour quality and no dependence of the heat transfer on ΔT is found for those test conditions. It can be assumed that a fully developed annular flow is then occurring and forced convection is the sole driving heat transfer mechanism.

Figure 3 shows the heat transfer coefficient measured when condensing R-410A at the same saturation temperature as R-134a and saturation pressure equal to 2420 kPa. R-125 experimental coefficients are reported in figure 4 at 100, 150, 200, 400 and 750 kg/(m^2 s). The refrigerant R-125 condensing at 40°C displays an operating saturation pressure equal to 2010 kPa and thus a reduced pressure $p_{RED} = 0.55$.

Measured trends for the three fluids are roughly the same, even if the value of the heat transfer coefficient under the same flow condition varies significantly. At 40 °C saturation temperature, 750 kg/(m^2 s) mass velocity and 0.5 vapour quality, R-134a presents the highest heat transfer performance during condensation, with the heat transfer coefficient equal to 6000 W/(m^2 K), while R-410A and R-125 have coefficients of 5000 and 3500 W/(m^2 K) respectively.

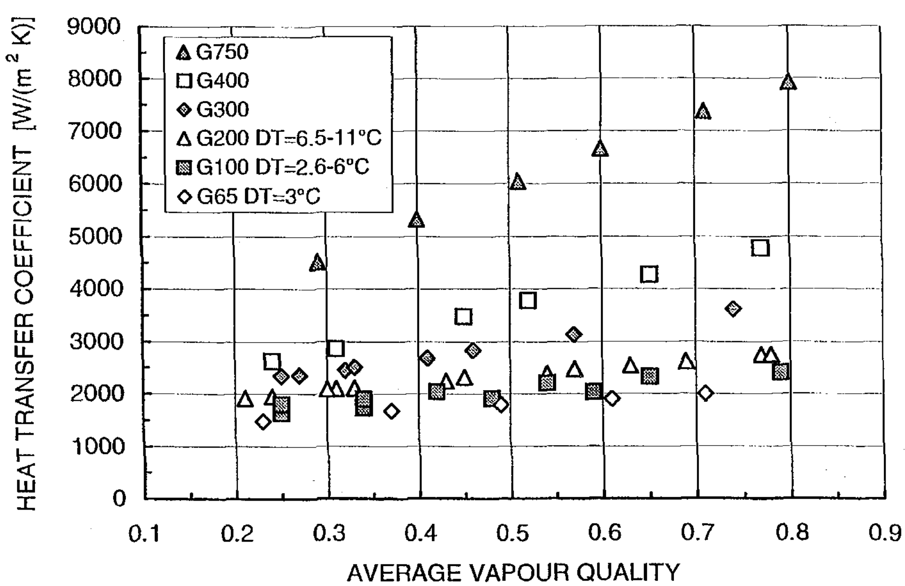

Figure 2. Experimental heat transfer coefficients vs. vapour quality for refrigerant 134a at $T_{sat} = 40±3$°C.

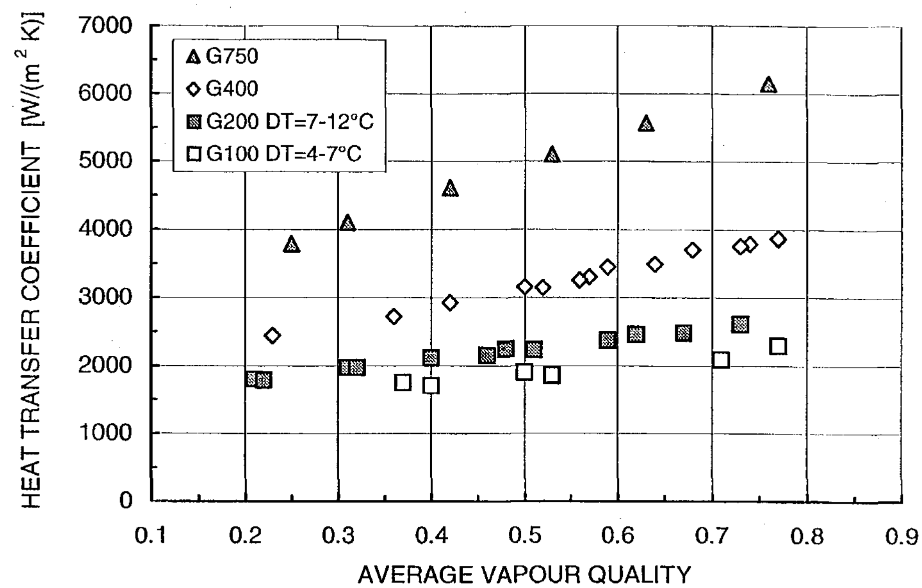

Figure 3. Experimental heat transfer coefficients vs. vapour quality for refrigerant 410A at $T_{sat} = 40 \pm 2°C$.

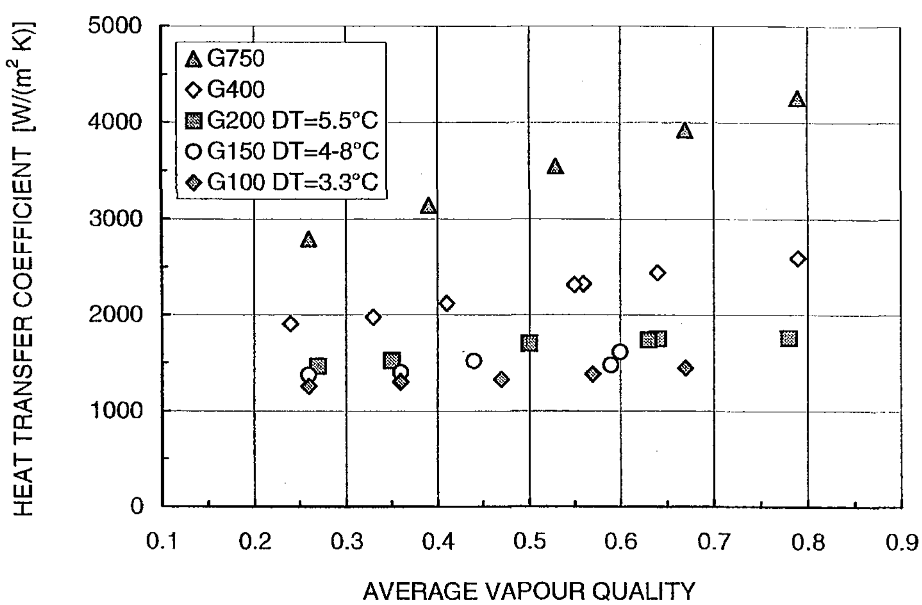

Figure 4. Experimental heat transfer coefficients vs. vapour quality for refrigerant 125 at $T_{sat} = 40 \pm 2°C$.

COMPARISON AGAINST MODELS

As it can be seen by plotting the data points on a flow pattern map (Cavallini et al., 1999), experimental flow conditions presented here cover both annular and wavy-stratified flows. For the case of annular flow, experimental heat transfer is compared against the Kosky and Staub (1970) model, which is based on the momentum - heat transfer analogy. Their analysis allows to calculate the heat transfer coefficient during condensation inside a smooth tube assuming annular film and constant film thickness along the tube circumference. Applying the momentum – heat transfer analogy to calculate the liquid layer thermal resistance, one gets to the following expression for the heat transfer coefficient

$$h = \frac{q/A}{T_{sat} - T_w} = \frac{c_L \rho_L u_\tau}{T_\delta^+} = \frac{c_L (\rho_L \tau)^{0.5}}{T_\delta^+} \qquad (2)$$

where u_τ is the friction velocity, τ is the shear stress, assumed constant along the liquid film, T_δ^+ is a dimensionless parameter evaluated at the vapour-liquid interface. Assuming the Von Karman universal velocity distribution inside the pipe to hold for the liquid condensate layer, T_δ^+ can be written as a function of δ^+ :

$$T_\delta^+ = \delta^+ Pr_L \qquad \text{for } \delta^+ < 5$$

$$T_\delta^+ = 5\, Pr_L + 5 \ln [1 + Pr_L (\delta^+/5 - 1)] \qquad \text{for } 5 < \delta^+ < 30$$

$$T_\delta^+ = 5\, Pr_L + 5 \ln(1 + 5\, Pr_L) + 2{,}5 \ln(\delta^+/30) \qquad \text{for } \delta^+ > 30$$

where Pr_L is the Prandtl number of the liquid phase and the dimensionless film thickness $\delta^+ = \rho_L u_\tau \delta / \mu_L$. Kosky and Staub related δ^+ to the liquid layer Reynolds number $Re_L = G\, D\, (1-x) / \mu_L$:

$$\delta^+ = (Re_L / 2)^{0.5} \qquad \text{for } Re_L < 1145$$

$$\delta^+ = 0{,}0504\, Re_L^{\ 7/8} \qquad \text{for } Re_L > 1145$$

The interfacial shear stress is first determined:

$$\tau = (-dp_f/dz)\, D/4$$

where $-dp_f/dz$ is the frictional pressure gradient along the channel and D is the tube diameter. The frictional pressure gradient can be evaluated by using the equation proposed by Kosky and Staub themselves, or by adopting alternative procedures. As suggested by Cavallini et al. (1983), $(-dp_f/dz)$ appearing in the model is here calculated by using the Friedel (1979) equation.

When the flow is not fully annular, the above model cannot be used since the shear stress is not the sole driving mechanism anymore. The Jaster and Kosky (1976) equation is then used to calculate the heat transfer coefficient under hypothesis of gravity controlled condensation, by adopting the Rohuani (1969) correlation to calculate the void fraction.

After application of the Kosky and Staub analysis and the Jaster and Kosky model, the higher of the two values is taken as the predicted heat transfer coefficient. In Figure 5 calculated heat transfer coefficients are plotted versus experimental values of R-134a. The figure shows a good agreement between calculated and experimental heat transfer coefficients, with higher deviation at low flow rate, where the coefficient calculated by the Jaster and Kosky equation results higher than by assuming forced convection driven condensation.

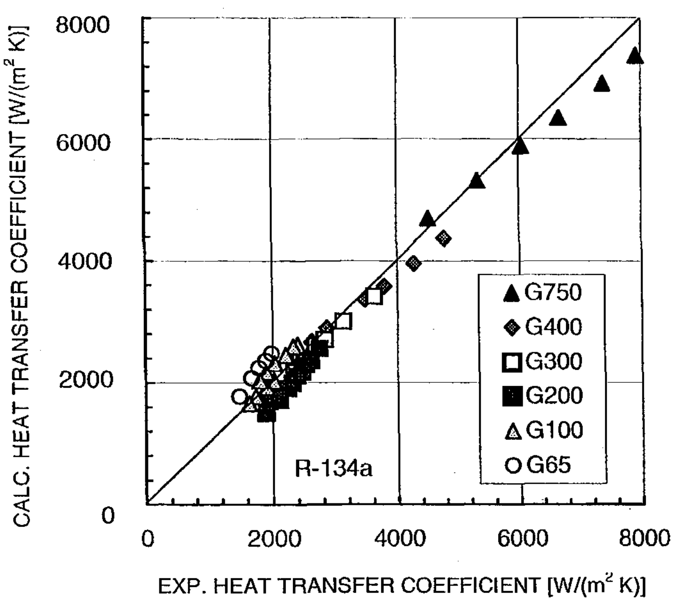

Figure 5. Calculated vs experimental heat transfer coefficients for R-134a: predictions by Kosky and Staub (1970) method with Jaster and Kosky (1976) equation.

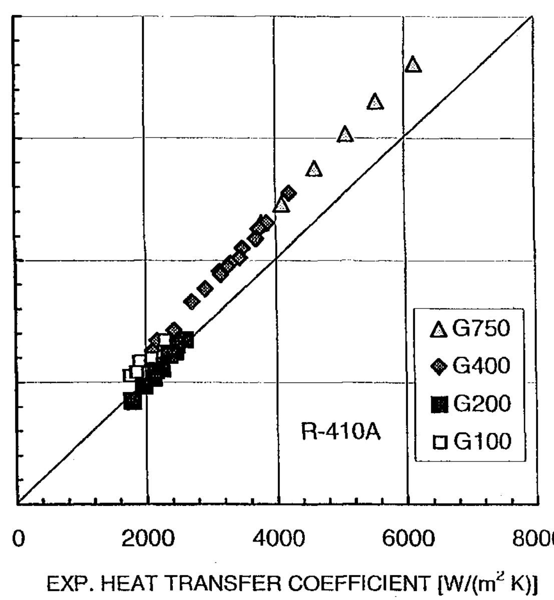

Figure 6. Calculated vs experimental heat transfer coefficients for R-410A: predictions by Kosky and Staub (1970) method with Jaster and Kosky (1976) equation.

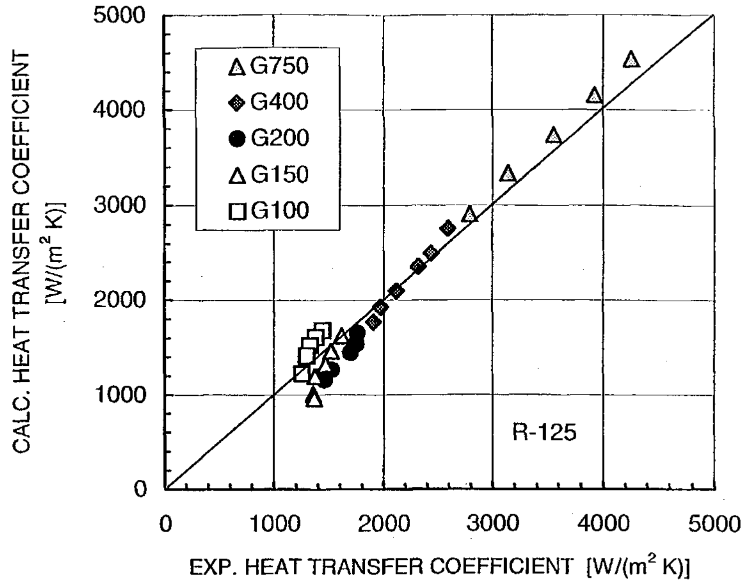

Figure 7. Calculated vs experimental heat transfer coefficients for R-125: predictions by Kosky and Staub (1970) method with Jaster and Kosky (1976) equation.

Regarding the R-134a data, the mean percent deviation MDA is around 7.8%, where

$$MDA = (1 / Np)\ \Sigma\ [\ |\ h_{CALC} - h_{EXP}\ |\ /\ h_{EXP}\ ] \cdot 100$$

with Np being the number of experimental points. A worst agreement between calculated and experimental values is found for R-410A, as depicted in Figure 6, with a mean percent deviation equal to 15%. High mass velocity data points (400 and 750 kg/(m^2 s)) are about 18% overestimated by the predicting model, while a smaller deviation is found at lower mass velocity (200 kg/(m^2 s)). A similar trend as for R-134a is shown in Figure 7, where R-125 calculated heat transfer coefficients are plotted against the experimental values. Mean deviation in this last case is around 8%.

COMPARISON AMONG FLUIDS

Heat transfer performance of these three fluids can easily be compared with one another from Figures 2 to 4. It can be seen for instance that at 400 kg/(m^2 s) and 50% vapour quality the R-134a coefficient is around 3800 W/(m^2 K), the R-410A coefficient is equal to 3200 W/(m^2 K) and the R-125 coefficient is around 2250 W/(m^2 K). When referred to the R-22 heat transfer coefficient measured by the present authors as reported in Cavallini et al. (1999) (3550 W/(m^2 K)), R-134a seems to perform 7% better, while R-410A presents a 10% underperformance and R-125 a 37% underperformance. By looking at the condensation heat transfer this way (clearly misleading), only disadvantages of using high pressure fluids are underlined.

Such conclusions can easily be rejected by arguing that these fluids have different pressure drop behavior. Thus, a fair comparison among these fluids must account for different saturation temperature drops at same mass velocity (Fabbretti et al., 1998). By considering an acceptable value for the saturation temperature drop during condensation, a performance evaluation of the different refrigerants is here carried out by comparing the heat transfer coefficient obtained at different mass velocities. The saturation temperature penalty is not to be referred to a constant tube length, but rather to the length needed for total condensation.

In the present work R-22 is chosen as the reference refrigerant, and condensation inside a smooth 8 mm ID tube at 40°C saturation temperature is considered. For R-22 at a mass velocity of 400 kg/(m^2 s), one can compute the heat transfer coefficient as a function of vapour quality only (an annular flow pattern is present in this situation). From the frictional pressure gradient along the condensing tube, one can also compute the frictional saturation temperature gradient dT_{sat}/dz as a function of vapour quality x (for simplicity's sake, refrigerant properties are always considered at 40°C saturation temperature). Being:

$$dT_{sat}/dp = T\,(1/\rho_G - 1/\rho_L)\,/\,i_{LG} \qquad -(dp_f/dz) = \Phi_{LO}^2\, 2\, f_{LO}\, G^2 / (\rho_L D) \qquad -(dz/dx) = i_{LG}\, G\, D\, /\, (4\, h\, \Delta T_{DR})$$

where Φ_{LO}^2 and f_{LO} are the frictional multiplier and the friction factor respectively, both referred to the liquid phase with total flow rate, it is possible to compute, at the set condition, the value of the dimensional group $(dT_{sat}/dx)\ \Delta T_{DR}$ as a sole function of vapour quality x. When considering a different fluid within the same pipe and at the same initial saturation temperature, the mass velocity giving rise to the same value of the parameter $(dT_{sat}/dx)\ \Delta T_{DR}$ as for refrigerant 22 can be calculated at different values of vapour quality; it comes out that this mass velocity is only a very weak function of vapour quality x. The heat transfer coefficient can then be computed for the various refrigerants as a function of vapour quality, at values of mass velocity G giving rise to the same value of the parameter $(dT_{sat}/dx)\ \Delta T_{DR}$ as found for the benchmark fluid R-22 at G=400 kg/(m^2 s).

The results of the above computation are reported in figure 8. Thanks to the good results given by the Kosky and Staub model in the heat transfer prediction, this same model is used to calculate the condensation coefficient in the present discussion. For calculating saturation pressure drop, the Friedel (1979) model is used. As reported by Cavallini et al. (2000), Friedel model gives an acceptable prediction of pressure gradient during condensation of R-22, R-134a, R-410A and R-125, although it overestimates by 10 to 30% these last two fluids experimental data points. In the graph of figure 8 the heat transfer coefficients of the other refrigerants are plotted as ratios to the heat transfer coefficient of the benchmark fluid R-22 at G_{R-22}=400 kg/(m^2 s); those ratios are only weak functions of the vapour quality x. The different plots represent, as compared to R-22 at G=400 kg/(m^2 s), the values of the heat transfer coefficients obtainable with the other refrigerants, subject to the constraint of the same saturation temperature (frictional) depression under the same driving temperature difference (saturation minus tube wall). The mass velocities (G in [kg/(m^2 s)]) pertaining to the different refrigerants are also reported in the graph. It can be observed that the variation with vapour quality is small; reference to a mean value is certainly an acceptable approximation.

The graph in figure 8 evidences the advantage of the high pressure fluids: R-125 outperforms R-22 by 10-15%, while R-134a displays a penalty of about 10% as compared to R-22. The diagram highlights the big advantage (according to the set criterion) in using R-410A, which outperforms R-22 by 70%, thanks both to the high operating pressure and to the high value of the liquid phase thermal conductivity (due to the component R-32). The set criterion implies exploiting the better performance of the high pressure fluids by decreasing the heat transfer surface, and the actual gain depends of course on the relative weight the condensation heat transfer coefficient has on the value of the overall heat transfer coefficient of the condenser.

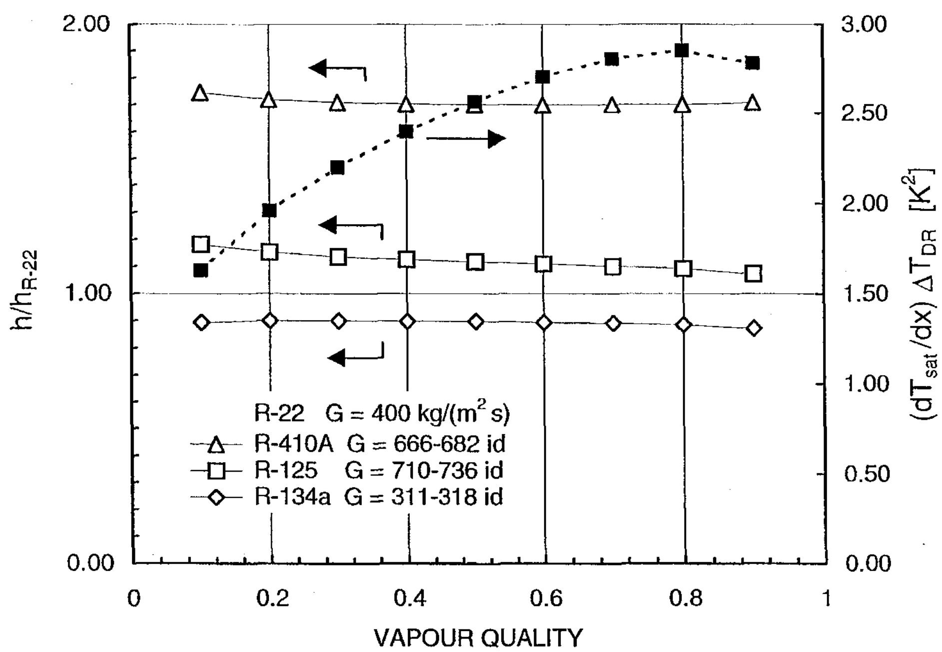

Figure 8. R-134a, R-410A and R-125 condensation heat transfer coefficient referred to the R-22 coefficient when condensing at 400 kg/(m^2 s) mass velocity in a 8 mm ID tube, at T_{sat}=40°C. Mass velocity, referred to as G, is obtained at constant value of $(dT_{sat}/dx)\ \Delta T_{DR}$. Parameter $(dT_{sat}/dx)\ \Delta T_{DR}$ is plotted over vapour quality and mass velocity range is reported.

Table 2: Mass velocity and condensation heat transfer coefficient for R-134a, R-410A and R-125 referred to the case of R-22 condensing at 300, 400 and 500 kg/(m^2 s) mass velocity in a 8 mm ID tube, at T_{sat}=40°C.

		R-134a	**R-410A**	**R-125**
G_{R-22} = 300 kg/(m^2 s)	**G/G$_{R-22}$**	0.78-0.79	1.67-1.71	1.78-1.84
	h/h$_{R-22}$	0.88-0.90	1.70-1.74	1.06-1.17
G_{R-22} = 400 kg/(m^2 s)	**G/G$_{R-22}$**	0.78-0.80	1.67-1.71	1.78-1.84
	h/h$_{R-22}$	0.87-0.90	1.70-1.75	1.07-1.18
G_{R-22} = 500 kg/(m^2 s)	**G/G$_{R-22}$**	0.78-0.80	1.66-1.70	1.78-1.84
	h/h$_{R-22}$	0.88-0.90	1.70-1.75	1.08-1.19

The advantage of the high pressure fluids can of course be exploited in different ways, besides decreasing the heat transfer area, that is:

- reducing the frictional saturation temperature drop with unchanged heat transfer area and driving temperature difference, advantaging the energy efficiency of the equipment;
- reducing the driving temperature difference with unchanged heat transfer area and frictional saturation temperature drop, again advantaging energy efficiency;
- or suitably compromising among the various possibilities.

Mass velocities and heat transfer coefficients are listed in Table 2 as ratios to the relative values of the benchmark fluid R-22 at 300, 400 and 500 kg/(m^2 s) R-22 mass velocity. Although the predicting model was verified against experimental data up to 750 kg/(m^2 s), in this analysis calculated results are shown for mass velocities of the high pressure fluids R-410A and R-125 up to 850 and 920 kg/(m^2 s) respectively. It can be seen that those ratios are not significantly dependent on the R-22 mass velocity considered as reference.

CONCLUSIONS

Local heat transfer coefficients were measured for R-134a, R-410A and R-125 in a horizontal smooth tube at an average saturation temperature of 40°C. At higher mass velocity, heat transfer coefficients increase linearly with vapour quality for all three fluids. Experimental data is successfully compared against the Kosky and Staub analysis for shear controlled condensation and the Jaster and Kosky equation for gravity driven condensation. When comparing the performances, a parameter is introduced to account for the saturation pressure drops. Based on equal saturation temperature drop, the high pressure refrigerant R-410A performs 70% better than R-22, while the lower pressure refrigerant R-134a presents 10% lower coefficient as compared to R-22. By assuming a maximum value for the saturation temperature drop, related values of mass velocity change for different fluids. This saturation temperature drop criterion can provide a useful parameter for the design of a condenser when moving from R-22 to new high pressure fluids, such as R-410A.

REFERENCES

1. Cavallini A., Del Col D., Doretti L., Longo G.A., Rossetto L., Condensation of R-22 and R-407C inside a horizontal tube, *20th International Congress of Refrigeration, IIR/IIF*, Sydney, September 19-24, 1999.
2. Cavallini A., Del Col D., Doretti L., Longo G.A., Rossetto L., Condensation pressure losses in smooth tubes, *3rd European Thermal Sciences Conf.*, Heidelberg, September 10-13, 2000.
3. Cavallini A., Frizzerin S., Rossetto L., Forced convection condensation of refrigerants inside a vertical annulus, *IchemE Symposium Series No.75*, pp. 309-322, 1983.
4. Fabbretti V., Fornasieri E., Foroni A., R-22 and R-410A: compared heat transfer performances in coils, *AICARR Free '98*, pp.195-207, 1998 (in Italian).
5. Friedel L., Pressure drop during gas/vapor-liquid flow in pipes, *Int. Chem. Eng.*, July, vol.20, p.352-367, 1980.
6. Jaster H., Kosky P.G., Condensation heat transfer in a mixed flow regime, *Int. J. of Heat Mass Transfer*, vol. 19, pp. 95-99, 1976.
7. Kosky, P.G., Staub F.W., Local condensing heat transfer coefficients in the annular flow regime. *AIChE J.*, Vol.17, 1971.
8. Rouhani S.Z., Subcooled void fraction, *AB Atomenergi Sweeden, Internal Rept. AE-RTV841*, 1969.
9. Sardesai, R.G., Owen, R.G., Pulling, D.J. Pressure drop for condensation of a pure vapour in downflow in a vertical tube. Proc. of the 8th Int. Heat Trans. Conf., Munchen, p.139-145, 1982.
10. Traviss, D.P., Rohsenow, W.M., Baron, A.B., Forced convection inside tubes: A heat transfer equation for condenser design. *ASHRAE Trans.*, Vol.79, pp.157-165, 1972.